fluids

MDPI

Article

Simulation of Relaxation Processes in Hypersonic Flows with One-Temperature Non-Equilibrium Model

Anton Karpenko [1], Semen Tolstoguzov [2] and Konstantin Volkov [3,*]

[1] Faculty of Mathematics and Mechanics, St Petersburg State University, St. Petersburg 198504, Russia; akarpenko@mail.ru
[2] Faculty of Aerospace Engineering, Baltic State Technical University, St. Petersburg 190005, Russia; stolstoguzov@mail.ru
[3] Institute of Hydrodynamics and Control Processes, St Petersburg State Marine Technical University, St. Petersburg 190121, Russia
* Correspondence: dsci@mail.ru

Abstract: Steady-state one-dimensional flows of five-component air behind a normal shock wave are considered with a one-temperature model. A mathematical model is formulated to describe the relaxation of a five-component air mixture with a one-temperature non-equilibrium approximation. A numerical study of non-equilibrium flows of a reacting five-component air mixture behind shock waves at different heights and velocities of free flow is performed. The contribution of different types of reactions to the overall relaxation of the mixture is discussed, and the distributions of macro-parameters of the flow behind the shock wave front are calculated. The lengths of the relaxation zones behind the shock wave front are compared at different initial conditions. Calculations are performed for the standard model of atmosphere.

Keywords: aerodynamics; hypersonic flow; shock wave; physical and chemical processes; chemical kinetics; relaxation



Citation: Karpenko, A.; Tolstoguzov, S.; Volkov, K. Simulation of Relaxation Processes in Hypersonic Flows with One-Temperature Non-Equilibrium Model. *Fluids* **2023**, *8*, 297. https://doi.org/10.3390/fluids8110297

Academic Editors: Mikhail V. Chernyshov and D. Andrew S. Rees

Received: 19 August 2023
Revised: 30 October 2023
Accepted: 8 November 2023
Published: 10 November 2023



Copyright: © 2023 by the authors. Licensee MDPI, Basel, Switzerland. This article is an open access article distributed under the terms and conditions of the Creative Commons Attribution (CC BY) license (https://creativecommons.org/licenses/by/4.0/).

1. Introduction

Finding solutions to the practical problems of high-speed aerodynamics leads to the need to study physical and chemical processes in air flows behind shock waves. The air behind the shock wave formed near an aircraft during its entry into the atmosphere is heated to high temperatures [1]. As a result of air heating, there is an excitation of internal degrees of freedom, energy exchange between molecules and processes of dissociation and ionization [2–5]. These processes are characterized by a significant imbalance between different degrees of freedom of molecules (thermally non-equilibrium gas). The need to study non-equilibrium flows of gas mixtures also arises in flows formed in rocket engine nozzles and when reproducing experimental conditions in shock tubes [6–8].

The development of models of different levels of physical complexity is dictated by the relationships between the characteristic relaxation times of processes occurring in high-temperature air. In high-temperature and high-enthalpy flows, the excitation of the internal degrees of freedom of molecules and chemical reactions leads to the violation of thermodynamic equilibrium. In this case, the relaxation processes leading to the establishment of equilibrium states proceed at different rates, some of which are comparable with the characteristic times of change in flow quantities. At high temperatures, the characteristic relaxation time of the translational degrees of freedom, τ_t, is of the order of the mean free path τ_0, and the relations $\tau_r \sim 5\tau_0$ are satisfied for the relaxation time of the rotational and vibrational degrees of freedom and $\tau_v \sim 1000\tau_0$ [9]. A specific feature of the flow behind shock waves is the significant difference between the relaxation times of different degrees of freedom. In air components at high temperatures, the time to establish equilibrium in translational and rotational degrees of freedom is much shorter than the time of vibrational and chemical

relaxation [10]. Taking into account the relationships between the characteristic times of kinetic processes, mathematical models of various levels of complexity have been developed that describe high-temperature air flows under different non-equilibrium conditions [3].

Models designed to describe non-equilibrium mixtures and based on the introduction of a common temperature do not take into account the effects of interaction between different vibrational modes. In many cases, the one-temperature approximation does not provide an adequate description of vibrationally non-equilibrium air flows and leads to significant differences in temperature and mixture composition found within the multi-temperature approximation. In particular, the application of the approximate approach leads to an underestimated length of the relaxation zone compared to modelling with the full model [11].

The most detailed and rigorous approach to the description of relaxation processes is a level-by-level approach based on the coupled solution of the equations for the populations of the vibrational levels of molecules and the densities of atoms together with the Euler equations [12,13]. The theory of relaxation processes in multi-component reacting gas mixtures, taking into account the level-by-level kinetics, was developed in [2,3] using the Chapman–Enskog method generalized for strongly non-equilibrium gases. Difficulties that arise in the numerical study of the level-by-level kinetics in flows of multi-component mixtures are associated with the need to solve a large number of equations for the populations of the vibrational levels of all molecular components of the mixture together with the equations for macro-parameters. The high computational costs and the presence of a large number of coefficients characterizing all kinds of energy exchanges between different types of oscillations make it difficult to use this approach in practice. In particular, when describing the vibrational spectra of molecules in a five-component model of air with a model of anharmonic oscillators, the model contains 122 equations for the populations of vibrational levels, the numerical densities of atoms, together with equations for macro-parameters [2,3].

In multi-temperature models, the distributions of parameters are characterized by different temperatures of translational and vibrational degrees of freedom [14,15]. Multi-temperature models make it possible to reduce the number of unknown functions and equations to be solved. The equations for a large number of populations of vibrational levels with multi-temperature descriptions are reduced to several equations for the vibrational temperatures of molecules of different chemical types. The multi-temperature approach seems to be more rigorous with respect to the simplified one-temperature approximation, without leading to significant difficulties in numerical simulation compared to the level-by-level approach [16–19]. The effect of vibrational excitation and dissociation of nitrogen and oxygen molecules in the flows of binary mixtures N_2/N and O_2/O in nozzles is studied with the level-by-level approach [13] and multi-temperature approximation [20]. The model of two-temperature physico-chemical kinetics taking into account the ionization process behind the front of a strong shock wave is considered in [21].

To find the dissociation rate coefficients of diatomic molecules, the Trinor–Marron model [22], Park model [23], as well as the model proposed in [24] are used. A comparison of the experimental values of reaction rate coefficients in reacting mixtures containing carbon dioxide molecules is presented in [25]. Various approaches to modelling physical and chemical processes in high-temperature air are discussed in [26]. The source terms in the equations of level kinetics in the five-component air model and the rate coefficients of exchange reactions behind shock waves are given in [27,28]. The macro-parameters of the flow and their change with distance from the shock wave front weakly depend on the chosen model of transition rate coefficients (the maximum difference is 3%). The choice of the energy exchange model has the greatest influence on the vibrational distributions at the beginning of the shock wave relaxation zone. With distance from the shock wave front, this influence becomes insignificant [29]. The processes of vibrational relaxation and thermally non-equilibrium dissociation of oxygen are discussed in [30].

Particular attention in the literature is given to issues related to the comparison of computational and experimental data [31]. The vibrational temperature of molecular oxy-

gen behind the shock wave with experimental measurements is compared in [32–34]. The results of the comparison show significant differences in flow quantities computed with various models. For some flow configurations, taking into account the effects of thermochemical non-equilibrium either has no effect or leads to small differences in the results obtained with equilibrium and non-equilibrium models [35]. A comparison of various models for describing the vibrational kinetics and chemical reactions in gas mixtures, as well as estimates of the effects of the initial vibrational nonequilibrium in a spatially homogeneous mixture and the influence of the vibrational excitation of gas molecules in free flow on the flow quantities behind the shock wave front are given in [36,37]. Such results show the importance of evaluating the various effects of vibrational and chemical non-equilibrium on flow parameters [11,38]. The results of verification of theoretical models of dissociation, exchange chemical reactions and vibrational relaxation are reported in [36].

There are practically no experimental data for such regimes. On the other hand, there is a wide range of theoretical models that make it possible to calculate the characteristics of chemical reactions at different levels of complexity. It is difficult to carry out experiments to study the relaxation zone behind shock waves at high velocities in air. The development of a simplified approach for describing high-temperature air flows that takes into account non-equilibrium effects and is suitable for performing parametric calculations in solving problems of hypersonic aerodynamics seems to be an important task. In this study, non-equilibrium flows of a reacting five-component air mixture consisting of N_2, O_2, NO, N, O behind a shock wave at different heights and at different velocities of free flow are simulated. To assess the applicability of the equilibrium thermodynamics model for calculating the macro-parameters behind the shock wave, the lengths of the relaxation zones are considered at various initial conditions. The results of flow simulation with a one-temperature model are compared with the results of numerical calculations with the equilibrium thermodynamics model. Calculations are performed for the standard model of atmosphere. The practical importance of the results presented is based on saving computational resources. The application of the model developed is less challenging in terms of computational time and memory requirements than more complex mathematical models.

2. Components of Air and Chemical Reactions

A five-component air mixture, consisting of N_2, O_2, NO, N, O, is considered. Dissociation reactions of diatomic molecules, recombination reactions and exchange chemical reactions occur in air mixture. In this case, the processes of ionization and excitation of electronic degrees of freedom are not taken into account, since the temperature range is considered in which the effect of these processes on the flow parameters is weaker than the effect of chemical reactions [2,39]. When considering flows of multi-component air mixtures, it is necessary to take into account not only the dissociation of molecules, but also exchange chemical reactions (Zeldovich exchange reactions) leading to the formation of nitric oxide molecules. The choice of the model of chemical exchange reactions plays an important role in the description of nonequilibrium kinetics in shock-heated air [29].

It is assumed that the following kinetic processes occur in five-component air:

— dissociation and recombination

$$N_2 + M \leftrightarrows N + N + M; \quad (1)$$

$$O_2 + M \leftrightarrows O + O + M; \quad (2)$$

$$NO + M \leftrightarrows N + O + M; \quad (3)$$

— exchange reactions

$$N_2 + O \leftrightarrows NO + N; \quad (4)$$

$$O_2 + N \leftrightarrows NO + O. \quad (5)$$

Here, M is the particle involved in the collision (N_2, O_2, NO, N, O). At temperatures below 3000 K, exchange reactions prevail over dissociation reactions, and at temperatures above 5000 K, the situation changes to the opposite effect when the contribution of dissociation becomes predominant.

The vibrational energy of c molecules at the i level, ε_i^c, is represented as the sum of the vibrational and rotational energies and is calculated on the basis of the Morse anharmonic oscillator model [2]

$$\varepsilon_c^i = \varepsilon_c^0 + hc(\omega_e^c - \omega_e^c x_e^c - \omega_e^c x_e^c i)i, \tag{6}$$

where

$$\varepsilon_c^0 = hc\left(\frac{1}{2}\omega_e^c - \frac{1}{4}\omega_e^c x_e^c\right).$$

Here, h is Planck constant, c is speed of light, ω_e^c, $\omega_e^c x_e^c$ are spectroscopic constants characterizing the frequency and anharmonicity of molecular vibrations. The superscript takes the values $c = N_2, O_2, NO$. Molecular constants for the components of the air mixture, taken from [2,40], are given in Table 1, where D_c is the dissociation energy. The characteristic rotational temperature is found from the relation $\theta_{r,c} = h^2/(8\pi^2 k I_c)$, where k is the Boltzmann constant and I_c is moment of inertia.

Table 1. Molecular constants.

Component	ω_e^c, $\mathbf{s^{-1}}$	$\omega_e^c x_e^c$, $\mathbf{m^{-1}}$	D_c, K	$\theta_{r,c}$, R
N_2	235,857	1432	113,493.16	2.867
O_2	158,019	1198	59,368.44	2.063
NO	190,420	1407.5	75,541.39	2.399

Assuming that the distribution of molecules over vibrational levels is quasi-stationary and corresponds to the Boltzmann distribution, for the populations of the vibrational levels of the air components, we have the relation

$$n_c^i(T) = \frac{n_c}{Z_c^v(T)} \exp\left(-\frac{\varepsilon_c^i}{kT}\right).$$

The oscillatory partition function depends only on temperature and is represented as

$$Z_c^v(T) = \sum_i \exp\left(-\frac{\varepsilon_c^i}{kT}\right).$$

3. Equations for Macro-Parameters

The ongoing processes are divided into fast and slow. Fast processes in a wide temperature range include translational and rotational relaxation with characteristic times τ_t and τ_r. Other processes, such as intermode exchanges, translational-to-vibrational energy transitions, and dissociation/recombination reactions, occur at times τ_{dis} and τ_{rec} comparable to the time of macro-parameters change, τ. In a thermally equilibrium mixture, all transitions of internal energy occur much faster than chemical reactions, and for the characteristic times of the processes the relation $\tau_t < \tau_r \ll \tau_{dis} \sim \tau_{rec} \sim tau$. To describe the relaxation of the mixture, a one-temperature description is used. In this case, the non-equilibrium chemical kinetics is considered under the conserved thermally equilibrium (Boltzmann) internal energy distributions of gas molecules.

In the kinetic theory of gas flows with fast and slow processes, the system of flow macroparameters is derived using additive collision invariants in the fast stage of the process [2]. The corresponding macro-parameters are the flow rate, the numerical densities of the mixture components, and the gas temperature. The system of equations for macro-

parameters, derived from the generalized Enskog–Chapman method, describing the flow of an inviscid gas, includes equations of chemical kinetics, equations of conservation of mass, momentum and energy.

The governing equations describing non-equilibrium air flows in the one-temperature approximation are considered. The determining macro-parameters of the flow are the numerical densities of molecules and atoms n_{N_2}, n_{O_2}, n_{NO}, n_N, n_O, gas temperature T and macroscopic velocity v.

The closed system of governing equations for macro-parameters contains equations of one-temperature non-equilibrium chemical kinetics and equations of conservation of momentum and total energy. In the case of a steady-state one-dimensional flow of an inviscid air, these equations have the following form [2]

$$
\begin{aligned}
&v\frac{dn_{N_2}}{dx} + n_{N_2}\frac{dv}{dx} = R_{N_2}^{2\leftrightarrow 2} + R_{N_2}^{2\leftrightarrow 3};\\
&v\frac{dn_{O_2}}{dx} + n_{O_2}\frac{dv}{dx} = R_{O_2}^{2\leftrightarrow 2} + R_{O_2}^{2\leftrightarrow 3};\\
&v\frac{dn_{NO}}{dx} + n_{NO}\frac{dv}{dx} = R_{NO}^{2\leftrightarrow 2} + R_{NO}^{2\leftrightarrow 3};\\
&v\frac{dn_{N}}{dx} + n_{N}\frac{dv}{dx} = R_{N}^{2\leftrightarrow 2} + R_{N}^{2\leftrightarrow 3};\\
&v\frac{dn_{O}}{dx} + n_{O}\frac{dv}{dx} = R_{O}^{2\leftrightarrow 2} + R_{O}^{2\leftrightarrow 3};\\
&\rho v\frac{dv}{dx} + \frac{dp}{dx} = 0;\\
&v\frac{dE}{dx} + (p+E)\frac{dv}{dx} = 0.
\end{aligned}
$$

Here, $\rho = \sum_M n_M m_M$ is mass density of the mixture, $p = nkT$ is pressure, $n = \sum_M n_M$ is number density of the mixture, E is the total energy per unit volume. The relaxation terms on the right-hand sides of the equations of chemical kinetics describe the change in the number densities of the mixture components due to molecular dissociation reactions and reverse recombination reactions.

The total energy of a unit volume is found from the relation

$$E = E_t + E_r + E_v + E_f,$$

where E_t, E_r, E_v, E_f are translational, rotational, vibrational energies and formation energy of mixture particles per unit volume. To calculate the components of the total energy, the relations are used

$$
\begin{aligned}
&E_t = \frac{3}{2}nkT;\\
&E_r = \sum_{c=N_2,O_2,NO} n_c kT;\\
&E_v = \sum_{c=N_2,O_2,NO} \sum_i (\varepsilon_c^i + \varepsilon_c^i) n_c^i(T);\\
&E_f = \sum_{d=N,O,NO} n_d \varepsilon_d^f.
\end{aligned}
$$

Here, ε_N^f, ε_O^f, ε_{NO}^f are the formation energies of NO molecule, and N and O atoms. The energies of formation of various components of the mixture (NO molecules, N and O atoms) are found from the relations

$$\varepsilon_N^f = \frac{1}{2}D_{N_2}, \quad \varepsilon_O^f = \frac{1}{2}D_{O_2}, \quad \varepsilon_{NO}^f = \frac{1}{2}(D_{N_2} + D_{O_2}) - D_{NO}.$$

The governing equations form a closed system of non-linear ordinary differential equations describing the one-dimensional flow of the air mixture, taking into account the reactions of exchange, dissociation and recombination. To integrate them, the implicit Gear method is applied. This approach has high accuracy and computational efficiency, allowing to solve stiff systems with variable order and integration steps.

4. Initial Conditions

In the one-temperature approximation, it is assumed that energy exchanges occur inside the shock wave front, and dissociation and recombination begin immediately behind its front [2,3]. The one-temperature approach assumes that only the chemical composition of the mixture is preserved at the shock wave front. When modelling relaxation behind the shock wave front, the parameters in free flow are given as initial conditions, pressure p_0 (or mixture number density n_0), mixture temperature T_0, Mach number M_0 (or gas velocity v_0) and the initial composition of the mixture. Then the parameters of the gas behind the shock front are calculated. The obtained values are used as initial ones in solving the system of equations describing the conservation laws.

To determine the parameters behind the shock wave, a system of mass, momentum, and total energy conservation equations is solved. For a steady-state one-dimensional flow at the shock wave front, the conditions of dynamic compatibility are satisfied

$$\rho v = \rho_0 v_0;$$

$$\rho v^2 + p = \rho_0 v_0^2 + p_0;$$

$$\frac{E+p}{\rho} + \frac{v^2}{2} = \frac{E_0 + p_0}{\rho_0} + \frac{v_0^2}{2}.$$

The subscript 0 corresponds to the parameters in free flow.

To find the parameters of the mixture behind the shock wave front, the conditions of dynamic compatibility are resolved. The obtained values of the flow quantities are used as initial conditions for equations written in the form of conservation conditions.

5. Relaxation Terms

To close the system of governing equations, it is necessary to express the relaxation terms, $R_c^{2\leftrightarrow 2}$ and $R_c^{2\leftrightarrow 3}$, in terms of flow macro-parameters. The subscript c corresponds to various air components.

The source terms $R_c^{2\leftrightarrow 2}$ describe changes in the number densities of molecules due to exchange Reactions (4) and (5) and have the following form [2]

$$R_{N_2}^{2\leftrightarrow 2} = n_{NO} n_N k_{NO\to N_2}^{N\to O} - n_{N_2} n_O k_{N_2\to NO}^{O\to N};$$

$$R_{O_2}^{2\leftrightarrow 2} = n_{NO} n_O k_{NO\to O_2}^{O\to N} - n_{O_2} n_N k_{O_2\to NO}^{N\to O};$$

$$R_{NO}^{2\leftrightarrow 2} = -R_{N_2}^{2\leftrightarrow 2} - R_{O_2}^{2\leftrightarrow 2};$$

$$R_N^{2\leftrightarrow 2} = -R_{N_2}^{2\leftrightarrow 2} + R_{O_2}^{2\leftrightarrow 2};$$

$$R_O^{2\leftrightarrow 2} = R_{N_2}^{2\leftrightarrow 2} - R_{O_2}^{2\leftrightarrow 2}.$$

Here, $k^{O\to N}_{N_2\to NO}(T)$ and $k^{N\to O}_{O_2\to NO}(T)$ are the rate coefficients of direct exchange reactions (temperature dependent), $k^{N\to O}_{NO\to N_2}(T)$ and $k^{O\to N}_{NO\to O_2}(T)$ are the rate coefficients of reverse Reactions (4) and (5) depending on temperature.

The source terms $R_c^{2\leftrightarrow 3}$ describe the processes of dissociation and recombination (1)–(3) and have the form [2]

$$R_{N_2}^{2\leftrightarrow 3} = \sum_{M=N_2,O_2,NO,N,O} n_M\left(n_N^2 k^M_{rec,N_2} - n_{N_2}k^M_{N_2,dis}\right);$$

$$R_{O_2}^{2\leftrightarrow 3} = \sum_{M=N_2,O_2,NO,N,O} n_M\left(n_O^2 k^M_{rec,O_2} - n_{O_2}k^M_{O_2,dis}\right);$$

$$R_{NO}^{2\leftrightarrow 3} = \sum_{M=N_2,O_2,NO,N,O} n_M\left(n_N n_O k^M_{rec,NO} - n_{NO}k^M_{NO,dis}\right);$$

$$R_{N}^{2\leftrightarrow 3} = -2R_{N_2}^{2\leftrightarrow 3} - R_{NO}^{2\leftrightarrow 3};$$

$$R_{N}^{2\leftrightarrow 3} = -2R_{O_2}^{2\leftrightarrow 3} - R_{NO}^{2\leftrightarrow 3}.$$

Here, $k^M_{N_2,dis}(T)$, $k^M_{O_2,dis}(T)$ and $k^M_{NO,dis}(T)$ are the rate coefficients of dissociation of molecules N_2, O_2, NO upon collision with particle M, depending on temperature, $k^M_{rec,N_2}(T)$, $k^M_{rec,O_2}(T)$ and $k^M_{rec,NO}(T)$ are the rate coefficients of recombination of atoms with formation of molecules N_2, O_2, NO depending on temperature.

To calculate one-temperature rate coefficients of direct exchange and dissociation reactions, the Arrhenius law is used, which is valid in a thermally equilibrium gas

$$k^M_{c,e}(T) = A_M T^n \exp\left(-\frac{E}{kT}\right),$$

where $E = E_{\alpha,c}$ or D_c is activation energy in case of exchange reactions and dissociation energy in case of decay reactions; A_M and n are constant factors, which are determined from experimental data or numerical calculations. The dissociation rate coefficients recommended in [40] and given in Table 2 are used in the calculations.

The rate coefficients of recombination and reverse exchange reactions are found using the ratios following from the principle of detailed balance [2]

$$k^M_{rec,N_2}(T) = k^M_{N_2,dis}(T)\left(\frac{m_{N_2}}{m_N^2}\frac{h^2}{2\pi kT}\right)^{3/2} Z^r_{N_2}(T)Z^v_{N_2}(T)\exp\left(\frac{D_{N_2}}{kT}\right);$$

$$k^M_{rec,O_2}(T) = k^M_{O_2,dis}(T)\left(\frac{m_{O_2}}{m_O^2}\frac{h^2}{2\pi kT}\right)^{3/2} Z^r_{O_2}(T)Z^v_{O_2}(T)\exp\left(\frac{D_{O_2}}{kT}\right);$$

$$k^M_{rec,NO}(T) = k^M_{NO,dis}(T)\left(\frac{m_{NO}}{m_N m_O}\frac{h^2}{2\pi kT}\right)^{3/2} Z^r_{NO}(T)Z^v_{NO}(T)\exp\left(\frac{D_{NO}}{kT}\right);$$

$$k^{N\to O}_{NO\to N_2}(T) = k^{O\to N}_{N_2\to NO}(T)\left(\frac{m_{N_2}m_O}{m_{NO}m_N}\right)\frac{Z^r_{N_2}(T)Z^v_{N_2}(T)}{Z^{rot}_{NO}(T)Z^v_{NO}(T)}\exp\left(\frac{D_{N_2}-D_{NO}}{kT}\right);$$

$$k^{O\to N}_{NO\to O_2}(T) = k^{N\to O}_{O_2\to NO}(T)\left(\frac{m_{O_2}m_N}{m_{NO}m_O}\right)\frac{Z^{rot}_{O_2}(T)Z^v_{O_2}(T)}{Z^r_{NO}(T)Z^v_{NO}(T)}\exp\left(\frac{D_{O_2}-D_{NO}}{kT}\right).$$

Here, $Z^r_c(T)$ is the partition function of the rotational degrees of freedom, $Z^v_c(T)$ is the partition function of the vibrational degrees of freedom. The partition function of the rotational degrees of freedom is found from the relation

$$Z_c^r(T) = \frac{T}{\sigma_c \theta_c^{rot}},$$

where θ_c^r is the characteristic rotational temperature, $\sigma_{N_2} = \sigma_{O_2} = 2$ and $\sigma_{NO} = 1$ are symmetry factors.

Table 2. Constants in Arrhenius equations.

Reaction	A, m^3/s	n	$E_{\alpha,c}$ or D_c, J
$N_2 + N_2 \longrightarrow N + N + N_2$	4.1×10^{-12}	-0.62	15.67×10^{-19}
$N_2 + O_2 \longrightarrow N + N + O_2$	1.5×10^{-11}	-0.68	15.67×10^{-19}
$N_2 + NO \longrightarrow N + N + NO$	1.5×10^{-11}	-0.68	15.67×10^{-19}
$N_2 + N \longrightarrow N + N + N$	1.0×10^{-11}	-0.68	15.67×10^{-19}
$N_2 + O \longrightarrow N + N + O$	4.0×10^{-12}	-0.54	15.67×10^{-19}
$O_2 + N_2 \longrightarrow O + O + N_2$	1.3×10^{-10}	-1	8.197×10^{-19}
$O_2 + O_2 \longrightarrow O + O + O_2$	5.3×10^{-11}	-1	8.197×10^{-19}
$O_2 + NO \longrightarrow O + O + NO$	1.1×10^{-10}	-1	8.197×10^{-19}
$O_2 + N \longrightarrow O + O + N$	1.1×10^{-10}	-1	8.197×10^{-19}
$O_2 + O \longrightarrow O + O + O$	1.5×10^{-10}	-1.05	8.197×10^{-19}
$NO + N_2 \longrightarrow N + O + N_2$	2.1×10^{-10}	-1	10.43×10^{-19}
$NO + O_2 \longrightarrow N + O + O_2$	2.0×10^{-10}	-1	10.43×10^{-19}
$NO + NO \longrightarrow N + O + NO$	1.0×10^{-10}	-1	10.43×10^{-19}
$NO + N \longrightarrow N + O + N$	4.0×10^{-10}	-1.1	10.43×10^{-19}
$NO + O \longrightarrow N + O + O$	4.0×10^{-10}	-1.1	10.43×10^{-19}
$N_2 + O \longrightarrow NO + N$	0.8×10^{-16}	0	5.175×10^{-19}
$O_2 + N \longrightarrow NO + O$	4.0×10^{-15}	-0.39	0.2×10^{-19}

6. Results and Discussion

The chemical reactions behind a normal shock wave at different altitudes and flight speeds are considered. It is assumed that the air in free flow consists only of nitrogen and oxygen molecules, $n_{N_2} = 0.79 n_0$, $n_{O_2} = 0.21 n_0$, where $n_0 = p_0/(kT_0)$ is total number density of the mixture in free flow. The flight speed varies from M = 10 to M = 16. The upper limit is due to the fact that at Mach numbers above 16, the temperature and pressure immediately behind the shock layer have values at which ionization processes have a significant effect on the flow quantities [26]. To determine the parameters of free flow at different flight altitudes, the model of standard atmosphere (ISO 2533) is applied. The standard atmosphere sets the average numerical values of the main atmospheric parameters for heights from −2000 m to 1200 km for latitude 45°32′33″, corresponding to the average level of solar activity.

6.1. Composition of Mixture

In the one-temperature approximation, it is assumed that equilibrium is established inside the front in translational, rotational, and vibrational degrees of freedom. The values of the Mach numbers behind the shock wave and the ratios of the values of the macroparameters before and behind the wave front are related by Rankine–Hugoniot conditions.

Dependencies of temperature, speed, and concentrations of mixture components N_2, O_2, N, O, NO on the longitudinal coordinate at different flight altitudes are shown in Figures 1–7.

With an increase in the Mach number of free flow, the temperature and velocity changes become much more significant and pass much faster. As the flight altitude increases, the temperature and velocity behind the shock wave decrease (Figures 1 and 2).

As the Mach number increases, the concentration of the N_2 and O_2 components in the air mixture behind the shock wave decreases, while the rate of concentration change increases (Figures 3 and 4). At a height of 10 km, the concentration of the components increases. However, at an altitude of 24 km, the concentration of the components decreases and continues to decrease with an increasing altitude.

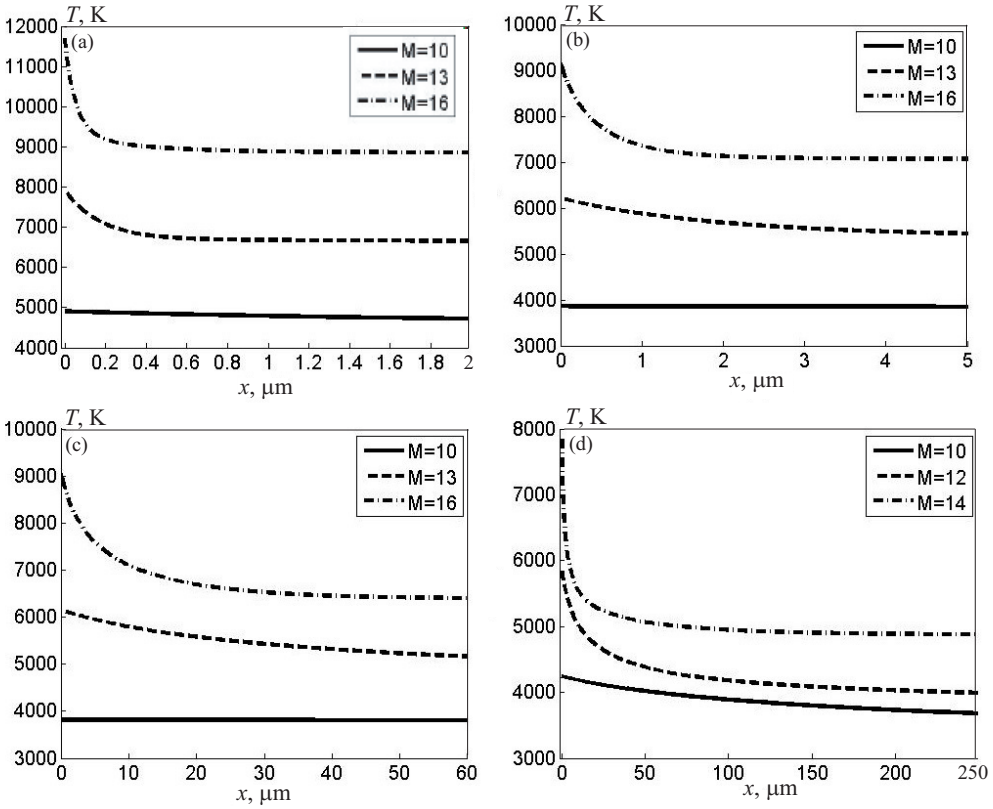


Figure 1. Dependencies of temperature on the longitudinal coordinate at different flight altitudes $h = 0$ km (**a**), $h = 10$ km (**b**), $h = 24$ km (**c**), $h = 60$ km (**d**).

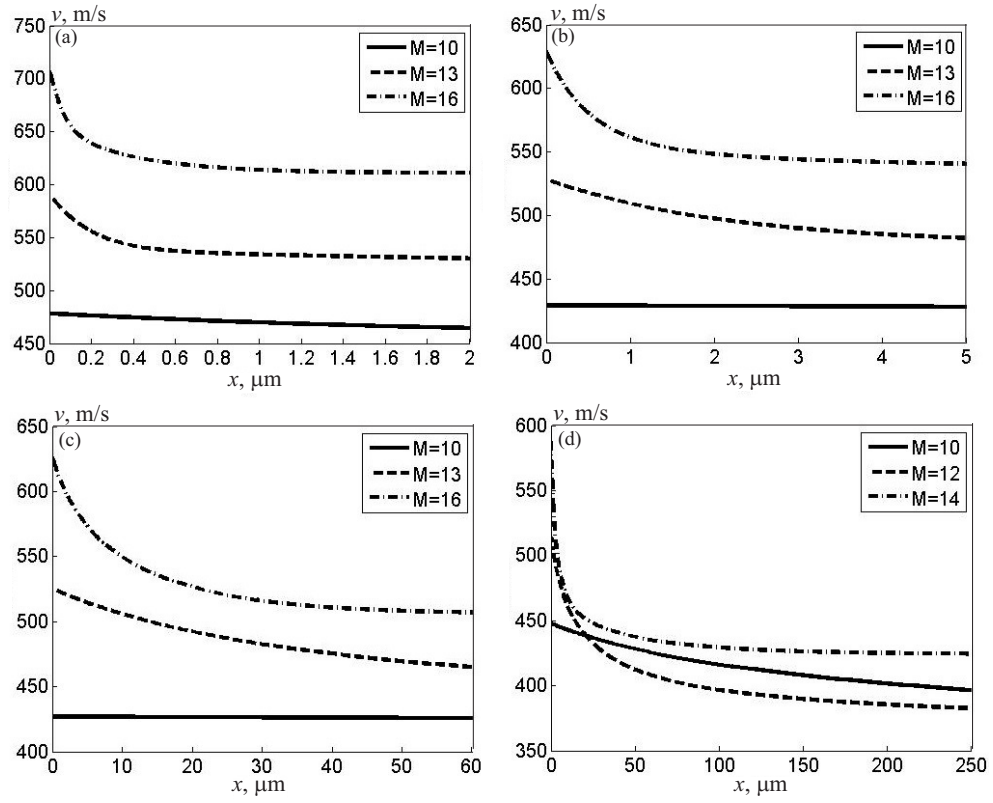


Figure 2. Dependencies of velocity on the longitudinal coordinates at different flight altitudes $h = 0$ km (**a**), $h = 10$ km (**b**), $h = 24$ km (**c**), $h = 60$ km (**d**).

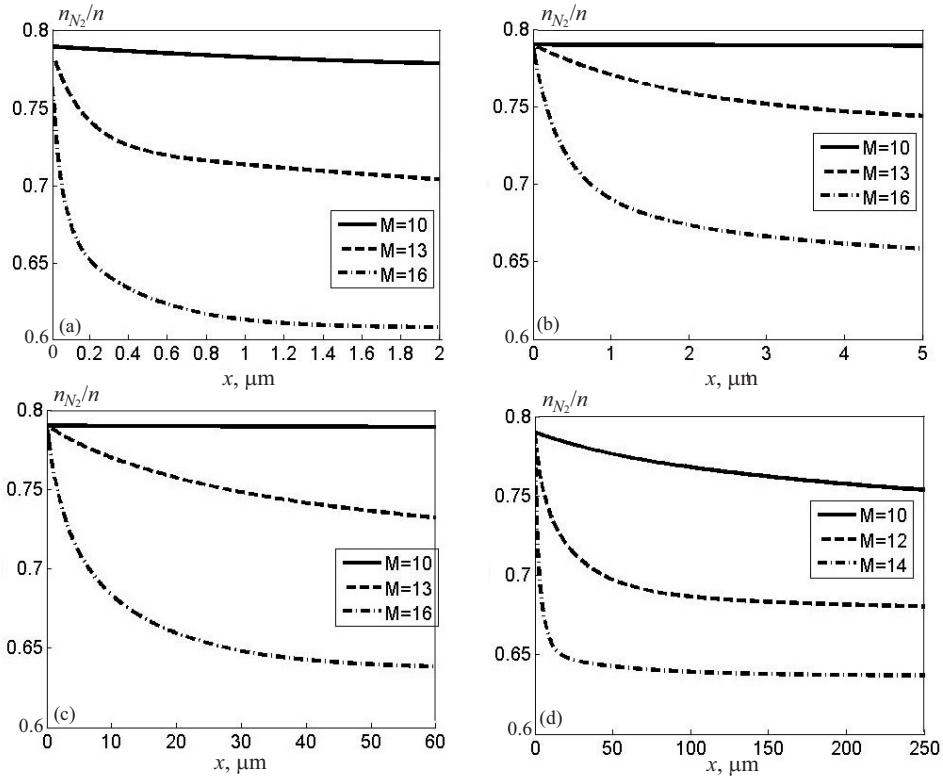


Figure 3. Dependencies of the n_{N_2} concentration on the longitudinal coordinate at different flight altitudes $h = 0$ km (**a**), $h = 10$ km (**b**), $h = 24$ km (**c**), $h = 60$ km (**d**).

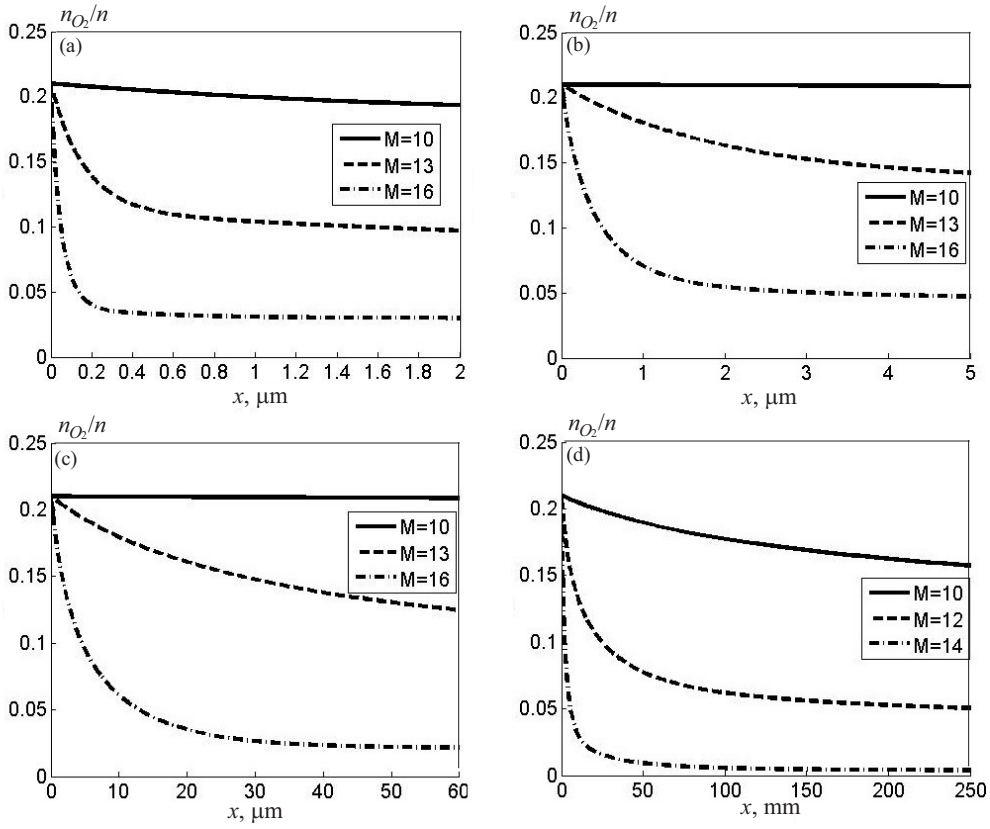


Figure 4. Dependencies of n_{O_2} concentration on the longitudinal coordinate at different flight altitudes $h = 0$ km (**a**), $h = 10$ km (**b**), $h = 24$ km (**c**), $h = 60$ km (**d**).

As the Mach number increases, the concentration of the *N* and *O* components in the air mixture increases behind the shock wave, and the concentration change gradient increases (Figures 5 and 6). As the altitude increases, the concentration of atomic nitrogen decreases. The concentration of atomic oxygen at a height of 10 km decreases, but at a height of 24 km an increase in concentration is observed.

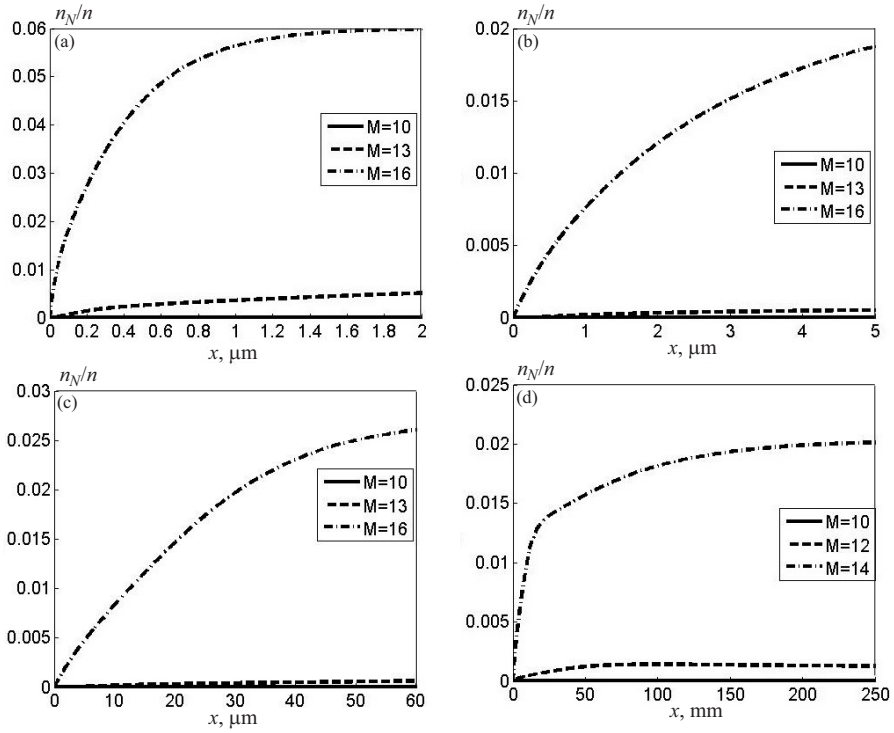


Figure 5. Dependencies of the concentration n_N on the longitudinal coordinate at different flight altitudes $h = 0$ km (**a**), $h = 10$ km (**b**), $h = 24$ km (**c**), $h = 60$ km (**d**).

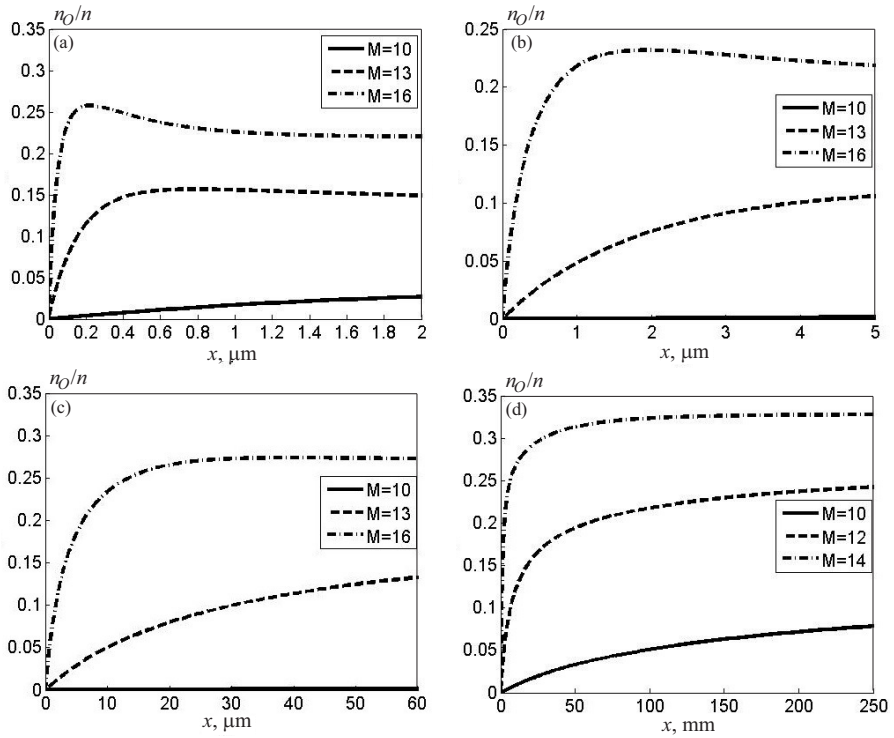


Figure 6. Dependencies of the n_O concentration on the longitudinal coordinate at different flight altitudes $h = 0$ km (**a**), $h = 10$ km (**b**), $h = 24$ km (**c**), $h = 60$ km (**d**).

At the initial stage, the main role is played by dissociation reactions leading to a decrease in the concentrations of nitrogen and oxygen molecules (n_{N_2} and n_{O_2}), the appearance of free atoms and the onset of direct exchange reactions with the formation of nitric oxide molecules (n_{NO}). With an increase in the number of atoms and molecules of nitric oxide, reverse exchange reactions are activated, and therefore the change in the number density of nitric oxide molecules occurs in a nonmonotonic manner. In general, nitric oxide molecules make up a relatively small fraction of the air mixture (Figure 7).

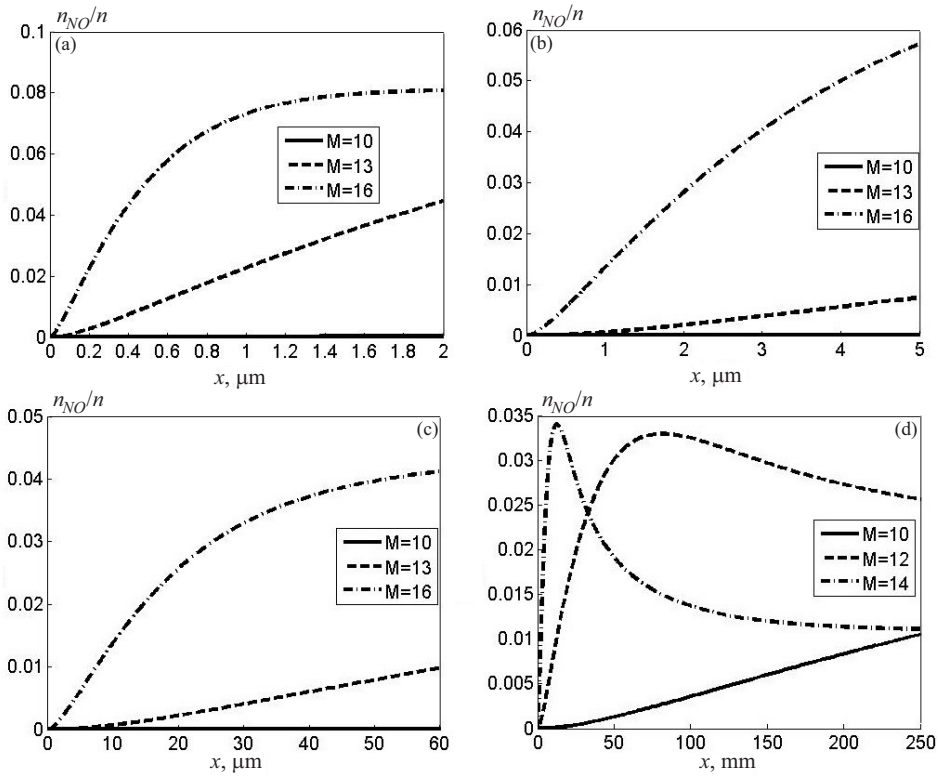


Figure 7. Dependencies of the n_{NO} concentration on the longitudinal coordinate at different flight altitudes $h = 0$ km (**a**), $h = 10$ km (**b**), $h = 24$ km (**c**), $h = 60$ km (**d**).

6.2. Length of Relaxation Region

The results of the numerical simulation make it possible to establish the role of chemical reactions in relaxation processes. The lengths of the zones behind the shock wave front, in which the flow parameters change by more than 1% of their final values—depending on the Mach number at different flight altitudes—are considered. In Figure 8, the y-axis shows the length of the relaxation zone in which the indicated parameter differs from the final result by 1%. The zone in which all flow quantities differ from the final result by 1% is called the relaxation zone. At the end of the relaxation zone, the distribution models lead to parameter values that are achieved at thermal and chemical equilibrium.

With an increase in the Mach number, the zone of chemical reactions decreases. On the one hand, the velocity behind the shock wave increases with an increasing Mach number, which leads to an increase in the relaxation zone. The pressure also increases, which leads to a decrease in the relaxation zone. Since the pressure increases much more than the velocity, the chemical reaction zone decreases. The establishment of macro-parameters occurs at a shorter distance than the establishment of some concentrations of the mixture components. The slowest is the establishment of the concentration of nitric oxide. The length of the relaxation zone is $x = 0.383$ mm at an altitude of $h = 0$ km, $x = 8.5$ mm at an altitude of $h = 10$ km, $x = 55$ mm at an altitude of $h = 24$ km, $x = 3211$ mm at an altitude of $h = 60$ km.

The lengths of the zones of change in the flow parameters behind the shock wave depending on the flight altitude at Mach numbers M = 10, 13, 16 are analysed. The solid

lines in Figure 9 show the lengths of the chemical reaction zones, where the error of the macroparameters (temperature, pressure, numerical density) relative to their final values exceeds 1%. The dashed-dotted lines show the lengths of the chemical reaction zones, where the error of the numerical components of the mixture relative to their final values exceeds 1%. The length of the zone of change in macro-parameters is much less than the length of the zone of change in the numerical densities of the mixture components.

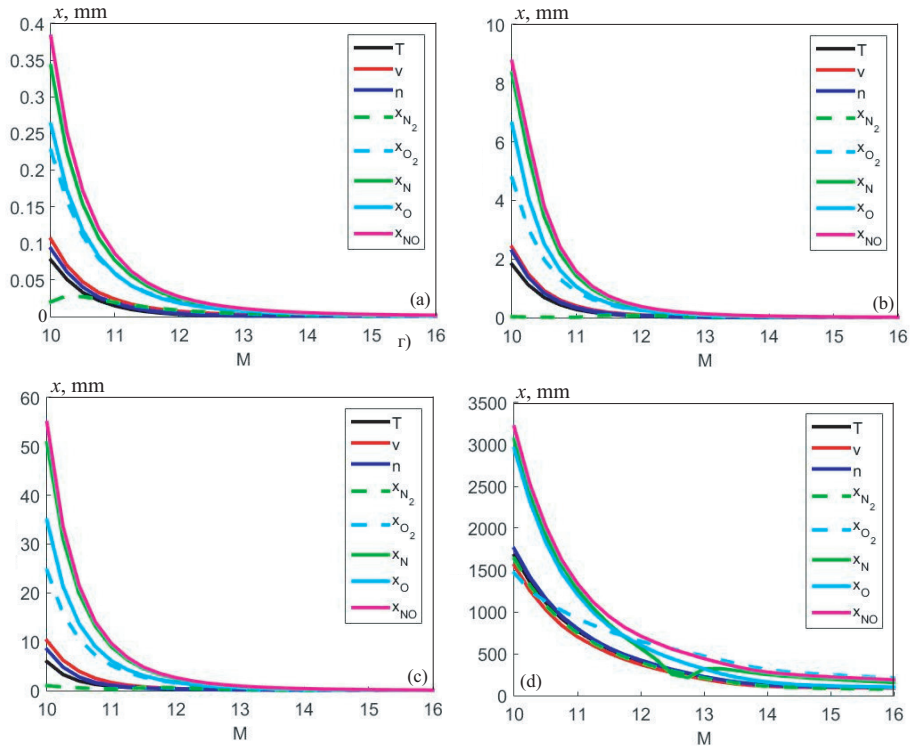


Figure 8. Relaxation zone length at height $h = 0$ km (**a**), 10 km (**b**), 24 km (**c**), 60 km (**d**).

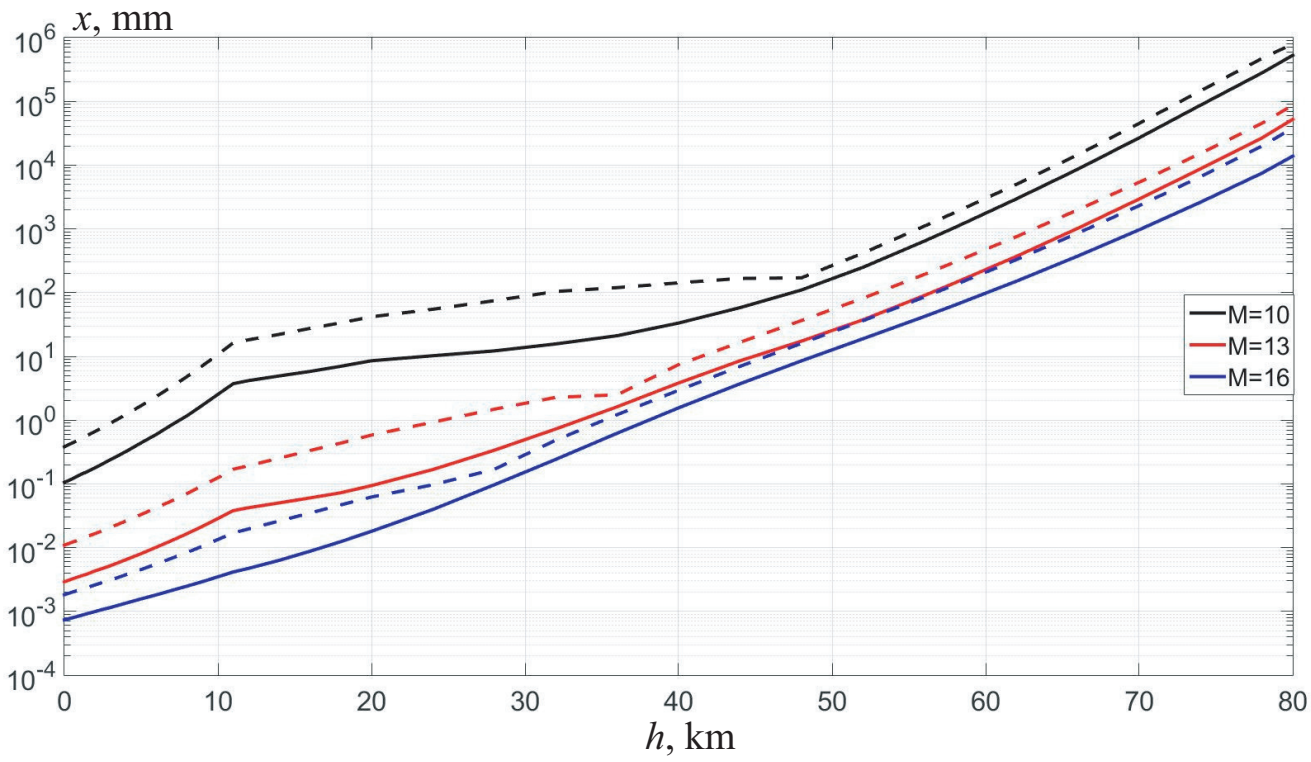


Figure 9. Lengths of the chemical reaction zones depending on the height at different Mach numbers.

At the Mach number M = 10, the conditional relaxation zone is already more than 1 mm at a height of 4 km above sea level (in this case, the length of the zone of change in macro-parameters at the same height is $x = 0.32$ mm). At a height of 10 km, the zone length is more than 1 cm ($x = 2.5$ mm for macro-parameters), at a height of 32 km it is more than 1 dm ($x = 1.57$ cm for macro-parameters), at a height of 60 km it is about 3 m ($x = 2.6$ m for macro-parameters). The length of the relaxation zones at the Mach number M = 10 exceeds the length corresponding to other Mach numbers.

At the Mach number M = 13, the length of the zone of change in flow parameters is more than 1 mm at an altitude of 25 km above sea level (while the length of the zone of change in macro-parameters at the same height is $x = 0.2$ mm). At a height of 42 km, the zone length is more than 1 cm ($x = 0.57$ cm for macro-parameters), at a height of 53 km it is more than 1 dm ($x = 0.47$ dm for macro-parameters) and at an altitude of 60 km it is about 4.7 dm ($x = 2.3$ dm for macro-parameters).

At the Mach number M = 16, the length of the zone of change in flow parameters is more than 1 mm at a height of 35 km above sea level (while the length of the zone of change in macro-parameters at the same height is $x = 0.5$ mm). At a height of 46 km, the zone length is more than 1 cm ($x = 0.58$ cm for macro-parameters), at a height of 57 km it is more than 1 dm ($x = 0.5$ dm for macro-parameters) and at a height of 60 km it is about 2.1 dm ($x = 1$ dm for macro-parameters).

An increase in the Mach number leads to an increase in the flow velocity directly behind the shock wave. However, the difference in velocity at the end of the relaxation zone is noticeable when the Mach number changes from 6 to 8 and amounts to about 10%. For $M > 8$, the differences between the velocity values do not exceed 3%, since in this case the temperature of the gas behind the shock wave increases, which leads to an additional loss of the initial kinetic energy and velocity due to active chemical reactions.

The obtained data on the lengths of the relaxation zone are given in Table 3 for various flight altitudes and Mach numbers of free flow.

Table 3. Relaxation zone length (in μm) depending on the flight altitude.

h, m	M = 10	M = 13	M = 16
0	0.382	0.010	0.00182
500	0.435	0.012	0.00199
1000	0.500	0.013	0.00217
1500	0.576	0.014	0.00236
2000	0.662	0.016	0.00260
2500	0.772	0.018	0.00285
3000	0.893	0.020	0.00309
4000	1.221	0.026	0.00375
5000	1.684	0.033	0.00453
6000	2.361	0.042	0.00553
7000	3.361	0.054	0.00683
8000	4.846	0.070	0.00842
9000	7.145	0.0942	0.010
10,000	10.680	0.124	0.013
11,000	16.358	0.169	0.016
12,000	18.195	0.192	0.019
14,000	22.156	0.253	0.026
16,000	27.493	0.333	0.034
18,000	33.598	0.435	0.046
20,000	41.799	0.582	0.062
24,000	54.895	0.928	0.096
28,000	74.700	1.483	0.169
32,000	104.143	2.274	0.48
36,000	119.754	2.494	1.218
40,000	142.343	7.409	2.936
50,000	262.711	54.330	24.078
60,000	2987.198	471.223	206.254

7. Comparison of Various Models

The results of the numerical calculations are compared with the results obtained with the multi-temperature approach and presented in [41]. The conditions in free flow correspond to an altitude of 48 km ($T_0 = 271$ K, $p_0 = 100$ Pa). The calculations are carried out at Mach numbers $M_0 = 10, 13, 16$ and the chemical composition of the air, consisting of 79% nitrogen and 21% oxygen ($n_{N_2} = 0.79n_0$, $n_{O_2} = 0.21n_0$, where n_0 is the total number density of the mixture in the oncoming flow).

Changes in temperature, flow velocity, relative numerical densities N_2, O_2, N, O, NO with distance from the shock wave front are shown in Figures 10–16. In the left pictures, the solid lines represent the simulation results obtained with the three-temperature model (it is based on the two-temperature Treanor distribution) and taken from [41], and the dash-dotted lines represent the solutions obtained with the one-temperature model (it is based on the equilibrium one-temperature Boltzmann distribution of anharmonic oscillators). In the right pictures, the solid lines show the distribution of quantities in the relaxation zone behind the shock wave front at the Mach number $M = 10$, the dash-dotted lines show the distribution of parameters in the relaxation zone behind the shock wave front at the Mach number $M = 13$, dotted lines show the distribution of parameters in the relaxation zone behind the shock wave front at Mach number $M = 16$. There is a good agreement between the results corresponding to different approaches. The values of the relative concentration NO found from the multi-temperature model exceed the corresponding values obtained with the one-temperature model (Figure 16).

The temperature and flow velocity distributions in the relaxation zone behind the shock wave show that the use of the one-temperature approximation leads to an underestimation of the temperature and velocity in the relaxation zone. This is more noticeable at high Mach numbers. In the one-temperature description, vibrational relaxation is a fast process, and the transition of translational energy into vibrational energy occurs inside the shock front. The difference between the temperatures found in the three-temperature and one-temperature approximations reaches 20% for $M = 16$. With distance from the front of the shock wave, the velocity decreases. At high Mach numbers in the oncoming flow, the speed decreases faster. The use of a single-temperature description leads to an underestimation of the rate by up to 24%.

Changes in the relative numerical densities of molecules and atoms with distance from the shock wave front show that the active dissociation of oxygen molecules, as well as the dissociation of nitrogen molecules, leads to the appearance of atoms and intense direct exchange reactions. With the accumulation of atoms and molecules of nitric oxide, the role of reverse exchange reactions increases, which leads to a non-monotonic change in the concentration of nitric oxide. The one-temperature model gives a significant underestimation of the densities of nitrogen and oxygen molecules, an overestimation of the densities of atoms and molecules of nitric oxide, and slows down the increase and decrease of nitric oxide molecules. This is explained by the fact that the one-temperature approximation does not describe the process of vibrational relaxation and the corresponding dissociation delay observed in a nonequilibrium gas both in theoretical calculations [2] and in experiments [9]. The differences between the flow parameters found in the three-temperature and one-temperature models decrease with distance from the shock wave front as equilibrium is approached. In the one-temperature approximation, there is no delay in reactions caused by vibrational relaxation, dissociation of molecules occurs immediately, and chemical and thermal equilibrium is reached faster.

The one-temperature approximation leads to underestimated temperatures behind the shock wave front, since it does not take into account the process of excitation of the vibrational degrees of freedom of molecules in the relaxation zone. The number densities of nitrogen and oxygen molecules and atoms obtained in the considered approaches have close values, and the maximum difference is about 5%. This is consistent with the data given in [29].

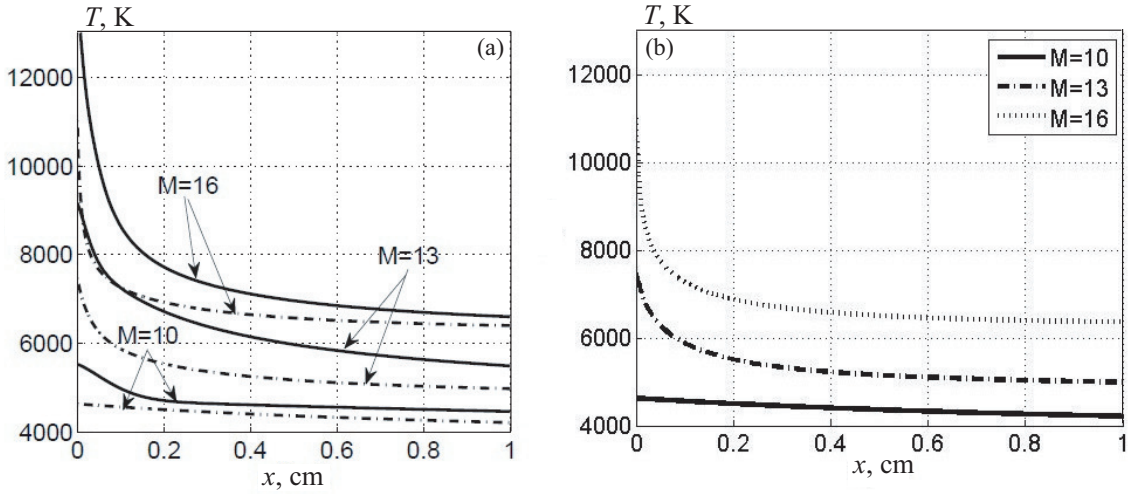


Figure 10. Dependencies of temperature on the longitudinal coordinate computed with multi-temperature (**a**) and one-temperature (**b**) models.

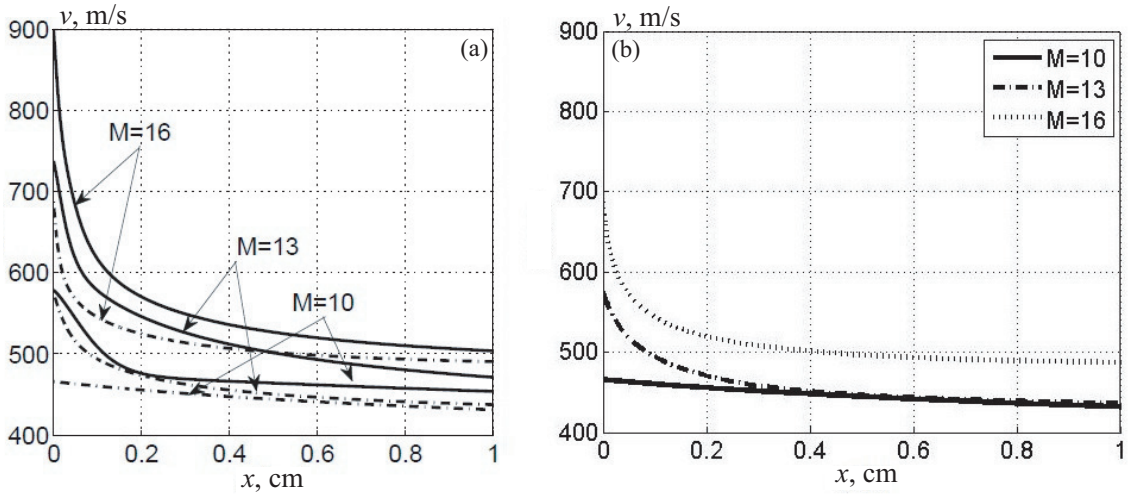


Figure 11. Dependencies of velocity on the longitudinal coordinate computed with multi-temperature (**a**) and one-temperature (**b**) models.

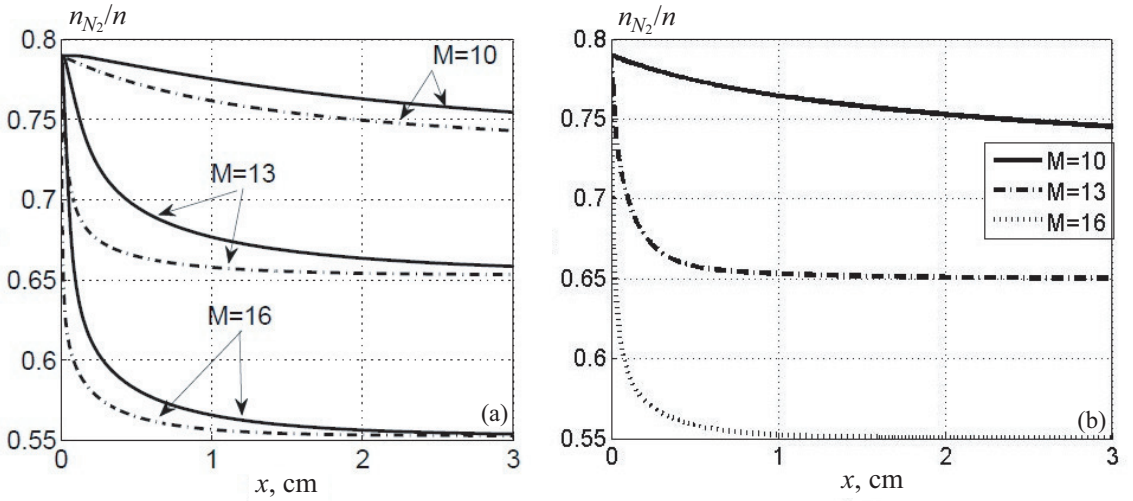


Figure 12. Dependencies of the concentration n_{N_2} on the longitudinal coordinate computed with multi-temperature (**a**) and one-temperature (**b**) models.

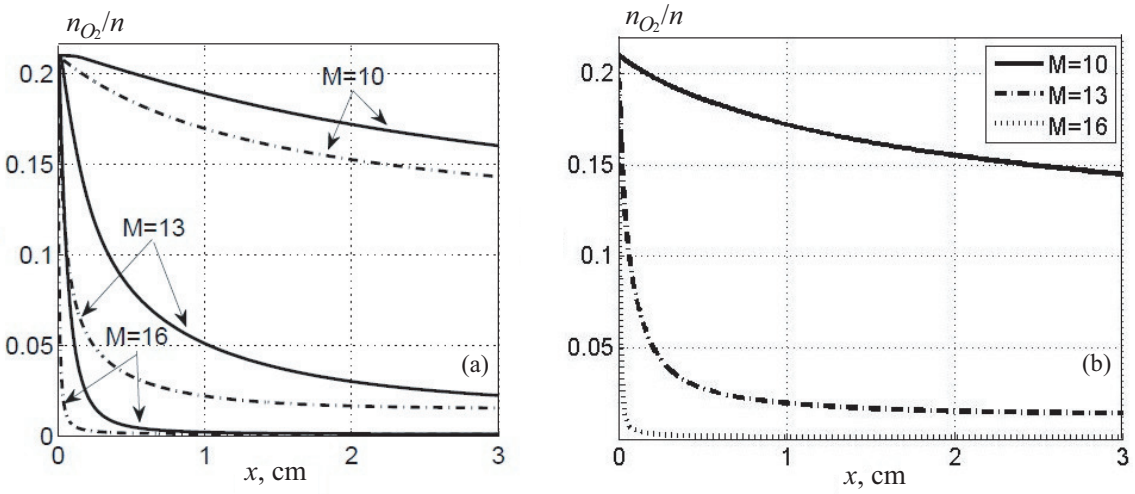


Figure 13. Dependencies of the concentration n_{O_2} on the longitudinal coordinate computed with multi-temperature (**a**) and one-temperature (**b**) models.

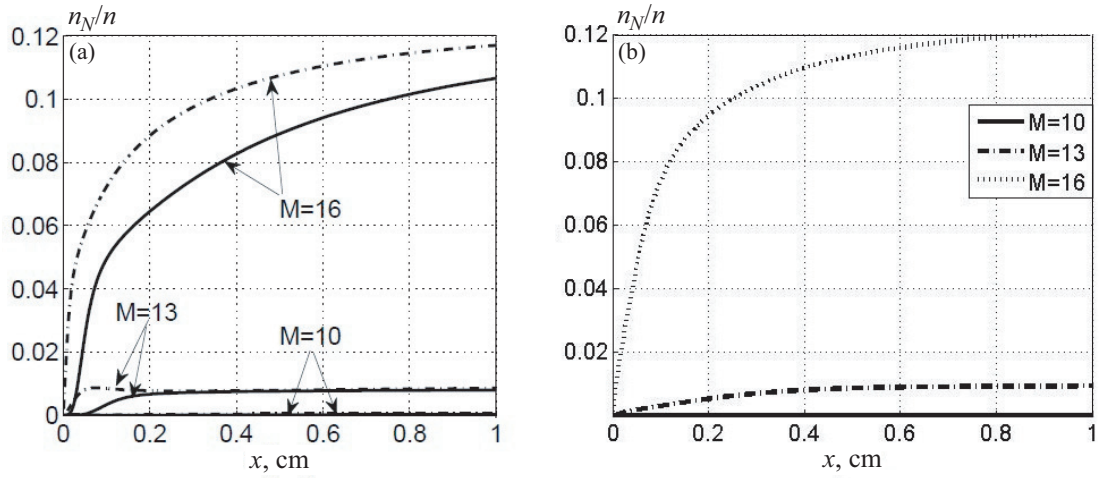


Figure 14. Dependencies of the concentration n_N on the longitudinal coordinate computedd with multi-temperature (**a**) and one-temperature (**b**) models.

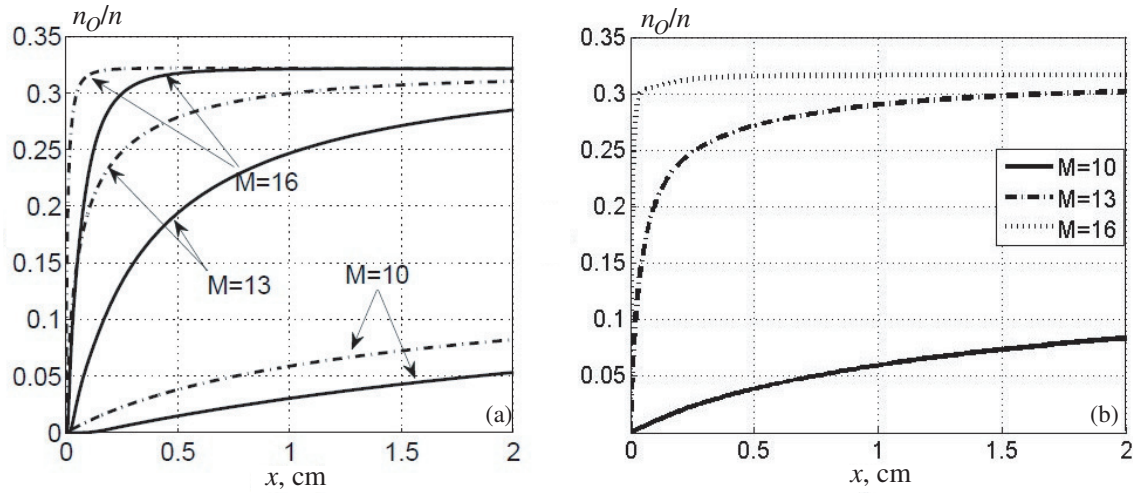


Figure 15. Dependencies of the concentration n_O on the longitudinal coordinate computed with multi-temperature (**a**) and one-temperature (**b**) models.

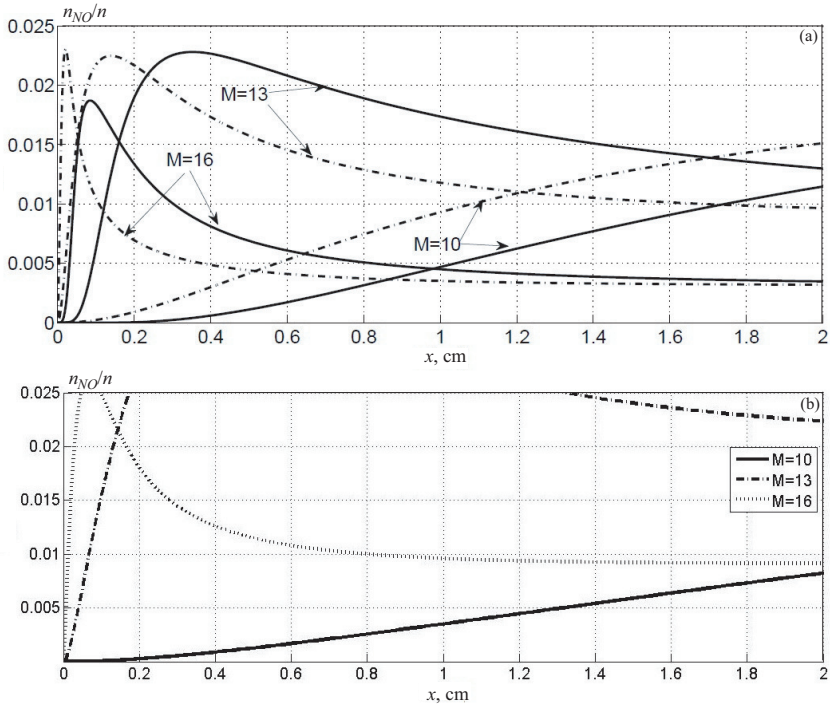


Figure 16. Dependencies of the concentration n_{NO} on the longitudinal coordinate computed with multi-temperature (**a**) and one-temperature (**b**) models.

The most active reaction is the reverse exchange reaction in the collision of N_2 molecules with O atoms, followed by exchange reactions involving oxygen molecules. In this case, near the shock wave front, the reverse reaction occurs more actively when NO molecules collide with O atoms, and as x increases, the forward reaction becomes more active when oxygen molecules collide with nitrogen atoms. The least active among the exchange reactions is the direct exchange reaction involving nitrogen molecules. Moreover, the most active dissociation of oxygen occurs upon collision with nitrogen molecules, and the least active occurs upon collision with oxygen molecules. Nitrogen dissociation also actively occurs in the collision of N_2 molecules with O_2 molecules, and less actively occurs in the collision of N_2 with N_2. In this case, the rate coefficients of nitrogen dissociation behind the shock wave remain lower than the rate coefficients of other reactions. One can also note a non-monotonic change in the rate coefficients of the direct Zeldovich reactions and dissociation with distance from the shock wave front, which is associated with a non-monotonic change in vibrational temperatures.

It is also interesting to compare the results computed with the results obtained with a more general approach to the simulation of hypersonic flows, for example Direct Simulation Monte Carlo (DSMC). The cases of stationary shock wave and assessment of various collision schemes are presented in [42]. At this stage, the results computed with the one-temperature model were compared with the temperature approach. Both sets of results were computed with similar computational algorithms.

8. Conclusions

A mathematical model of relaxation of a five-component inviscid air mixture behind the shock wave front is developed with one-temperature approximation. Numerical simulations of changes in gas-dynamic parameters behind shock waves at different heights and different Mach numbers of free flow have been carried out. The influence of the conditions in free flow on the distributions of macro-parameters and the relaxation rate is shown, and the lengths of the zones of change in the flow quantities behind the shock waves at different conditions are compared.

The simulations have shown that the length of the zone of change in the concentration of the components of the mixture exceeds the length of the zone of change in the macro-parameters of the flow behind the shock wave by a factor of 1.5–4. Therefore, in cases where there is no need to obtain the results of changing the concentration of the mixture components, the zone of numerical calculations of the flow can be reduced to the length of the zone of change in gas-dynamic variables. The length of the zone of change in the parameters of the flow behind the shock wave decreases with an increase in the velocity of free flow, since the pressure behind the shock wave front increases many times more than the velocity. With an increase in flight altitude, the length of the relaxation zone increases due to a decrease in density, pressure, and temperature in free flow.

Author Contributions: Conceptualization, methodology and software, validation, A.K.; formal analysis, investigation, writing—original draft preparation, writing—review and editing, K.V.; visualization, S.T.; supervision, K.V.; project administration, K.V. All authors have read and agreed to the published version of the manuscript.

Funding: The research is partially funded by the Ministry of Science and Higher Education of the Russian Federation as part of World-class Research Center program: Advanced Digital Technologies (contract No. 075-15-2020-903 dated 16 November 2020).

Data Availability Statement: Data are contained within the article.

Conflicts of Interest: The author declares no conflict of interest.

References

1. Dobrov, Y.; Karpenko, A.; Malkovsky, S.; Sorokin, A.; Volkov, K. Simulation of high-temperature flowfield around hypersonic waverider using graphics processor unit. *Acta Astronaut.* **2023**, *204*, 745–760. [CrossRef]
2. Nagnibeda, E.A.; Kustova, E.V. *Kinetic Theory of Transport and Relaxation Processes in Flows of Nonequilibrium Reacting Gases*; St Petersburg State University: St Petersburg, Russia, 2003.
3. Nagnibeda, E.; Kustova, E. *Non-Equilibrium Reacting Gas Flows. Kinetic Theory of Transport and Relaxation Processes*; Springer: Berlin/Heidelberg, Germany, 2009.
4. Emelyanov, V.N.; Karpenko, A.G.; Volkov, K.N. Simulation of hypersonic flows with equilibrium chemical reactions on graphics processor units. *Acta Astronaut.* **2019**, *163*, 259–271. [CrossRef]
5. Dobrov, Y.; Gimadiev, V.; Karpenko, A.; Volkov, K. Numerical simulation of hypersonic flow with non-equilibrium chemical reactions around sphere. *Acta Astronaut.* **2022**, *194*, 468–479. [CrossRef]
6. Park, C. Thermochemical relaxation in shock tunnels. *J. Thermophys Heat Transf.* **2006**, *20*, 689–698. [CrossRef]
7. Bazilevich, S.S.; Sinitsyn, K.A.; Nagnibeda, E.A. Non-equilibrium flows of reacting air components in nozzles. *AIP Conf. Proc.* **2009**, *1084*, 843–848.
8. Brykov, N.A.; Emelyanov, V.N.; Karpenko, A.G.; Volkov, K.N. Flows of real gas in nozzles with unsteady local energy supply. *Comput. Math. Appl.* **2021**, *81*, 702–724. [CrossRef]
9. Stupochenko, E.V.; Losev, S.A.; Osipov, A.I. *Relaxation Processes in Shock Waves*; Nauka: Moscow, Russia, 1965.
10. Losev, S.A.; Kovach, E.A.; Pogosbekyan, M.Y.; Sergievskaya, A.L. Modeling of physical and chemical processes in strong shock waves. *Phys. Chem. Kinet. Gas Dyn.* **2003**, *1*, 1–21.
11. Nagnibeda, E.A.; Sharafutdinov, I.Z. Three-temperature description of shock-heated air flows. *Phys. Chem. Kinet. Gas Dyn.* **2015**, *16*, 1–12.
12. Armenise, I.; Kustova, E. State-to-state models for CO_2 molecules: From the theory to an application to hypersonic boundary layers. *Chem. Phys.* **2013**, *415*, 269–281. [CrossRef]
13. Nagnibeda, E.A.; Papina, K.V. Non-equilibrium vibrational and chemical kinetics in air flows in nozzles. *Vestn. St. Petersburg State Univ.* **2018**, *5*, 287–299. [CrossRef]
14. Kunova, O.V.; Nagnibeda, E.A.; Sharafutdinov, I.Z. Non-equilibrium reaction rates in air flows behind shock waves. State-to-state and three-temperature description. *AIP Conf. Proc.* **2016**, *1786*, 150005.
15. Kosareva, A.; Nagnibeda, E.; Savelev, A. New multi-temperature reaction models for CO_2 containing mixtures and their applications. *Chem. Phys.* **2020**, *553*, 110718. [CrossRef]
16. Kustova, E.V.; Nagnibeda, E.A.; Shevelev, Y.D.; Syzranova, N.G. Comparison of different models for non-equilibrium CO_2 flows in a shock layer near a blunt body. *Shock Waves* **2011**, *21*, 273–287. [CrossRef]
17. Kustova, E.V.; Nagnibeda, E.A. Kinetic model for multi-temperature flows of reacting carbon dioxide mixture. *Chem. Phys.* **2012**, *398*, 111–117. [CrossRef]
18. Sharafutdinov, I.Z. Multi-temperature vibrational and chemical kinetics in air behind shock waves. *Vestn. Mosc. State Univ.* **2014**, *4*, 80–93.

19. Shevyrin, A.; Bondar, Y.; Kalashnikov, S.; Khlybov, V.; Degtyar, V. Direct simulation of rarefied high-enthalpy flow around the RAM C-II capsule. *High Temp.* **2016**, *54*, 383–389. [CrossRef]
20. Guy, A.; Bourdon, A.; Perrin, M.Y. Consistent multi-internal-temperatures models for nonequilibrium nozzle flows. *Chem. Phys.* **2013**, *420*, 15–24. [CrossRef]
21. Losev, S.A.; Makarov, V.N.; Pogosbekyan, M.Y. Model of physicochemical kinetics behind the front of a very strong shock wave in air. *Fluid Dyn.* **1995**, *2*, 169–182.
22. Marrone, P.V.; Treanor, C.E. Chemical relaxation with preferential dissociation from excited vibrational levels. *Phys. Fluids* **1963**, *6*, 1215–1221. [CrossRef]
23. Park, C.; Howe, J.T.; Jaffe, R.L.; Candler, G.V. Review of chemical-kinetic problems of future NASA missions. *J. Thermophys. Heat Transf.* **1994**, *8*, 9–23. [CrossRef]
24. Ibragimova, L.B.; Smekhov, G.D.; Shatalov, O.P. Dissociation rate constants under thermal equilibrium conditions. *Fluid Dyn.* **1999**, *1*, 181–186.
25. Shevelev, Y.D.; Syzranova, N.G. Influence of various models of chemical kinetics on supersonic carbon dioxide flow around blunt bodies. *Phys. Chem. Kinet. Gas Dyn.* **2007**, *5*, 1–21.
26. Emelyanov, V.N.; Karpenko, A.G.; Tolstoguzov, S.S.; Volkov, K.N. Analyzing models of air equilibrium composition calculation. *IOP Conf. Ser. Mater. Sci. Eng.* **2020**, *927*, 012064. [CrossRef]
27. Kunova, O.V.; Nagnibeda, E.A. State-to-state description of reacting air flows behind shock waves. *Chem. Phys.* **2014**, *441*, 66–76. [CrossRef]
28. Kunova, O.; Nagnibeda, E. On the influence of state-to-state distributions on exchange reaction rates in shock heated air flows. *Chem. Phys. Lett.* **2015**, *625*, 121–127. [CrossRef]
29. Kunova, O.V.; Nagnibeda, E.A. Level-by-level description of vibrational and chemical relaxation in air. *Vestn. St. Petersburg State Univ.* **2013**, *3*, 103–113.
30. Bykova, N.G.; Zabelinsky, I.E.; Ibragimova, L.B.; Sergievskaya, A.L.; Tunik, Y.V.; Shatalov, O.P. Investigation of vibrational relaxation and thermally nonequilibrium dissociation of O_2 molecules behind a shock wave front. *Phys. Chem. Kinet. Gas Dyn.* **2013**, *14*, 1–8.
31. Bourdon, A.; Annaloro, J.; Bultel, A.; Capitelli, M.; Colonna, G.; Guy, A.; Magin, T.E.; Munafo, A.; Perrin, M.Y.; Pietanza, L.D. Reduction of state-to-state to macroscopic models for hypersonics. *Open Plasma Phys. J.* **2014**, *7*, 60–75. [CrossRef]
32. Wysong, I.; Gimelshein, S.; Bondar, Y.; Ivanov, M. Comparison of direct simulation Monte Carlo chemistry and vibrational models applied to oxygen shock measurements. *Phys. Fluids* **2014**, *26*, 043101. [CrossRef]
33. Hao, J.; Wang, J.; Lee, C. Assessment of vibration–dissociation coupling models for hypersonic nonequilibrium simulations. *Aerosp. Sci. Technol.* **2017**, *67*, 433–442. [CrossRef]
34. Luo, H.; Alexeenko, A.; Macheret, S. Assessment of classical impulsive models of dissociation in thermochemical nonequilibrium. *J. Thermophys. Heat Transf.* **2018**, *85*, 2503–2504. [CrossRef]
35. Kianvashrad, N.; Knight, D. The effect of thermochemistry on prediction of aerothermodynamic loading over a double cone in a laminar hypersonic flow. In Proceedings of the 2018 AIAA Aerospace Sciences Meeting, Kissimmee, FL, USA, 8–12 January 2018; p. 1812.
36. Pogosbekyan, M.Y.; Sergievskaya, A.L. Modeling of the dynamics of molecular reactions and comparative analysis with theoretical models as applied to thermally nonequilibrium conditions. *Phys. Chem. Kinet. Gas Dyn.* **2014**, *15*, 1–7.
37. Kosareva, A.; Shoev, G. Numerical simulation of a CO_2, CO, O_2, O, C mixture: Validation through comparisons with results obtained in a ground-based facility and thermochemical effects. *Acta Astronaut.* **2019**, *160*, 461–478. [CrossRef]
38. Kustova, E.V.; Oblapenko, G.P.; Sharafutdinov, I.Z. Models of vibrational relaxation in nonequilibrium multi-temperature flows. *Phys. Chem. Kinet. Gas Dyn.* **2015**, *16*, 1–10.
39. Rusanov, V.D.; Fridman, A.A. *Physics of Chemically Active Plasma*; Nauka: Moscow, Russia, 1984.
40. Scanlon, T.J.; White, C.; Borg, M.K.; Palharini, R.C.; Farbar, E.; Boyd, I.D.; Reese, J.M.; Brown, R.E. Open-source direct simulation Monte Carlo chemistry modeling for hypersonic flows. *AIAA J.* **2015**, *53*, 1670–1680. [CrossRef]
41. Sharafutdinov, I.Z. Vibrational and Chemical Kinetics in Multi-Temperature Air Flows Behind Shock Waves. Ph.D. Thesis, Saint Petersburg State University, St Petersburg, Russia, 2016.
42. Shoja-Sani, A.; Roohi, E.; Stefanov, S. Homogeneous relaxation and shock wave problems: Assessment of the simplified and generalized Bernoulli trial collision schemes. *Phys. Fluids* **2021**, *33*, 032004. [CrossRef]

Disclaimer/Publisher's Note: The statements, opinions and data contained in all publications are solely those of the individual author(s) and contributor(s) and not of MDPI and/or the editor(s). MDPI and/or the editor(s) disclaim responsibility for any injury to people or property resulting from any ideas, methods, instructions or products referred to in the content.